ACTA IMEKO
ISSN: 2221-870X
September 2023, Volume 12, Number 3, 1 - 8

Evaluating the uncertainty of a virtual power quality disturbance generator and its use in power quality classifier evaluation

Bodan Velkovski[1], Marija Markovska[1], Zivko Kokolanski[1], Dimitar Taskovski[1], Vladimir Dimchev[1]

[1] *Ss. Cyril and Methodius University in Skopje, Faculty of Electrical Engineering and Information Technologies, Rugjer Boshkovik 18, PO Box 574, 1000 Skopje, North Macedonia*

ABSTRACT
This paper presents the metrological evaluation of a proposed virtual power quality (PQ) disturbance generator. It explains in detail the calibration and measurement uncertainty estimation procedures for the RMS voltage and frequency of the generator, presents the results, and discusses their implications. The results indicate that the measurement uncertainty of the generator is satisfactory for all reference points, making it suitable for generation of PQ signals for research purposes, particularly in the development, testing, and improvement of PQ event classifiers. Additionally, the paper introduces a virtual power quality disturbance classifier for real-time classification of PQ events and verifies its accuracy through testing using the proposed PQ disturbance generator.

Section: RESEARCH PAPER

Keywords: Power quality; measurement uncertainty; calibration; signal generator; virtual instrumentation

Citation: Bodan Velkovski, Marija Markovska, Zivko Kokolanski, Dimitar Taskovski, Vladimir Dimchev, Evaluating the uncertainty of a virtual power quality disturbance generator and its use in power quality classifier evaluation, Acta IMEKO, vol. 12, no. 3, article 18, September 2023, identifier: IMEKO-ACTA-12 (2023)-03-18

Section Editor: Marija Cundeva-Blajer, Ss. Cyril and Methodius University in Skopje, North Macedonia

Received February 2, 2023; **In final form** May 21, 2023; **Published** September 2023

Corresponding author: Bodan Velkovski, e-mail: bodan@feit.ukim.edu.mk

1. INTRODUCTION

Modern electrical grids face power quality (PQ) issues due to the heavy use of non-linear loads. The European standard EN 50160 [1] defines the voltage characteristics for normal operation in the public power distribution system in Europe. To address these problems, real-time monitoring and PQ disturbance classification systems are needed at various locations in the power grid. Advanced metering infrastructure and data analytics-based fault detection are crucial for power system security [2]. While some power grids have implemented power quality monitoring systems, they primarily rely on devices that only save raw voltage signals [3]-[9]. Other monitoring systems perform real-time processing and provide PQ indicators [10]-[13]. However, industrial grade instrumentation specifically designed for PQ monitoring is relatively expensive, hence the focus in recent years on development of virtual instrumentation-based PQ monitoring systems [14]-[19], as well as algorithms for fast and accurate detection and classification of PQ disturbances, such as the ones presented in [20], [21]. These solutions are decentralized and are more flexible and cost-effective, but require a large amount of curated PQ disturbance data, which can be difficult to obtain. There is a lack of publicly accessible good quality datasets of this kind [22]. Although there are commercially available PQ disturbance generators on the market which can be used to obtain this kind of data, they are too expensive for research purposes. Consequently, virtual instrumentation-based generators of PQ disturbances have been developed [23], [24], which can be used to obtain PQ data for research purposes.

In Section 2 of this paper, a virtual instrument for reproducing various combinations of standard power quality disturbances is presented. The virtual PQ generator is capable of reproducing voltage disturbances according to the European standard EN50160, providing a versatile and reliable tool for researching power quality issues. Section 3 of the paper presents a PQ disturbance classifier that is designed for real-time detection and classification of disturbances. The classifier is capable of recognizing 21 classes of single and combined PQ disturbances with high accuracy. To ensure the accuracy of the virtual PQ disturbance generator, Section 4 outlines a procedure

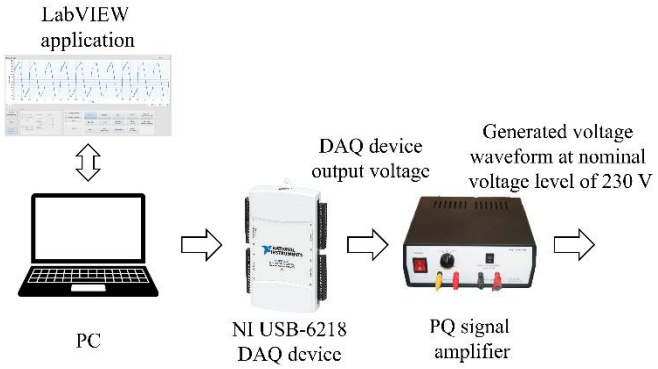

Figure 1. A schematic representation of the virtual PQ disturbance generator and its components.

for evaluating the measurement uncertainty components of the measurement setup. In Section 5, a comprehensive evaluation of the classifier's performance is conducted through testing its accuracy using the generator.

2. VIRTUAL POWER QUALITY DISTURBANCE GENERATOR

The main purpose of the designed virtual power quality disturbance generator, which is the subject of the metrological evaluation presented in this paper, is to generate and reproduce reference voltage signals and simulate standard voltage quality disturbances in accordance with the European standard EN50160 [1].

The generator mainly consists of two functional segments: a software application running on a personal computer and hardware components. The software application is developed in the LabVIEW graphical programming environment. The software realization of the virtual PQ generator, its functionalities, capabilities, and modes of operation are fully presented in [24]. The hardware components of the generator include a data acquisition (DAQ) device and a power quality signal amplifier. The DAQ device is used for hardware reproduction of the voltage waveforms generated by the software application. The device used is an NI USB 6218 multifunction acquisition device. The PQ signal amplifier is used to amplify the output voltage signal from the DAQ device to a nominal voltage level of 230 V. A detailed description of the design, functionality and characteristics of the PQ signal amplifier is given in [25].

A schematic representation of the PQ disturbance generator and its consisting hardware and software components is given in Figure 1.

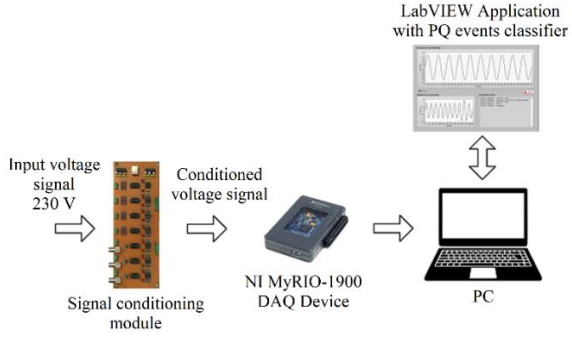

Figure 2. A schematic representation of the virtual PQ disturbance classifier and its components.

3. VIRTUAL POWER QUALITY DISTURBANCE CLASSIFIER

The PQ events classifier also consists of two functional segments: a software application running on a personal computer and hardware components: NI MyRIO-1900 DAQ device and a signal conditioning module. The signal conditioning module provides galvanic isolation, circuit protection, and filtering and adapts the input voltage signal from a nominal level of 230 V to a signal with parameters appropriate for the DAQ device. A detailed description of the design, functionality and characteristics of the signal conditioning module is given in [26]. A schematic representation of the PQ disturbance classifier and its components is given in Figure 2.

The software application is developed in LabVIEW and utilizes a producer-consumer architecture. The producer acquires voltage signals at a 3.2 kHz sampling frequency, while the consumer processes the data one frame at a time, with each frame consisting of 640 samples. This structure ensures that the producer does not add data to a full queue and the consumer does not retrieve data from an empty queue. In compliance with IEC 61000-4-30 [27], the basic measurement time interval for parameter magnitudes is a 10-cycle time interval for 50 Hz power systems or 12-cycle time interval for 60 Hz power systems, resulting in a measurement window of 200 ms. Thus, the producer acquires data every 200 ms, and the consumer's processing time must be less than 200 ms to ensure real-time implementation. In this implementation, the consumer's processing time is 5.54 ms, meeting the requirements for real-time implementation.

The consumer is a simple state machine with two states, "Classification" and "Stop." The "Classification" state enables real-time classification of input voltage signals through four steps, utilizing SubVIs as outlined in Figure 3. The first step is zero-crossing detection, which is an essential pre-processing step in PQ disturbance classification. It ensures that all signals in the feature extraction stage have similar phases, directly impacting the classifier's accuracy. The zero-crossing detection is implemented in the LabVIEW software application deployed on the real-time target device and is based on comparing successive values in a sequence. The second step is the feature extraction, achieved through the use of a discrete wavelet transform, based on the extraction of optimal feature combinations outlined in [28]. The third step is classification, where an optimized random forest approach is utilized. Research in [29] has shown that this approach provides higher classification accuracy compared to other methods for both pure signals and signals accompanied by noise. It is capable of classifying 21 classes of single and combined PQ disturbances, including those obtained as a combination of four disturbances. The classes and their labels are listed in Table 1. The final step of the "Classification" state is disturbance logging, providing continuous updates on the application's user interface for the type of disturbance, time, and

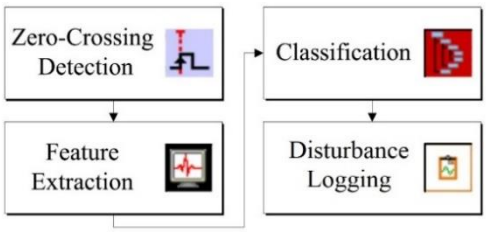

Figure 3. Real-time classification flowchart.

Table 1. Classes of PQ disturbances.

PQ disturbance	Class label
Pure	D1
Sag	D2
Swell	D3
Interruption	D4
Transient/Impulsive/Spike	D5
Oscillatory transient	D6
Harmonics	D7
Harmonics + Sag	D8
Harmonics + Swell	D9
Flicker	D10
Flicker + Sag	D11
Flicker + Swell	D12
Sag + Oscillatory transient	D13
Swell + Oscillatory transient	D14
Notch	D15
Harmonics + Sag + Flicker	D16
Harmonics + Swell + Flicker	D17
Harmonics + Sag + Oscillatory transient	D18
Harmonics + Swell + Oscillatory transient	D19
Harmonics + Sag + Flicker + Oscillatory transient	D20
Harmonics + Swell + Flicker + Oscillatory transient	D21

date of occurrence. Additionally, the application allows for saving raw voltage signals for further power quality analysis and for continuous classifier training to increase its accuracy. The state machine's "Stop" state is activated when the consumer is waiting for a new set of data.

4. CALIBRATION AND MEASUREMENT UNCERTAINTY ESTIMATION

The metrological evaluation of the implemented PQ generator involves conducting a calibration and estimating measurement uncertainty. The procedures for the calibration and calculation of measurement uncertainty, as well as the measurement uncertainty components, are presented in the following section.

The measurement uncertainty estimation is performed according to the recommendations in the Guide to the Expression of Uncertainty in Measurement [30], defined by the International Organization for Standardization. The procedure is divided into two segments: estimation of RMS voltage uncertainty and estimation of frequency uncertainty. Another approach to estimating the uncertainty would be by using the Monte Carlo Method [31]. However, the GUM approach was chosen instead, due to the model's relative simplicity, avoiding the need for a random number generator and the computational time requirements of Monte Carlo simulations.

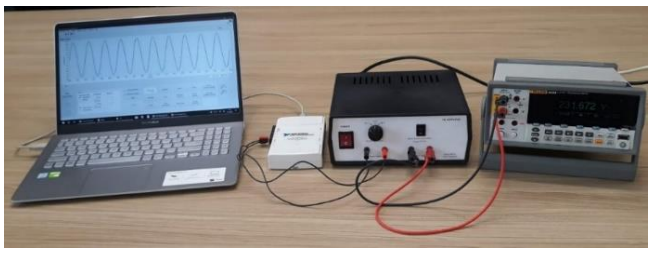

Figure 4. Experimental system used for calibration of the virtual PQ disturbance generator.

4.1. Voltage Uncertainty

The measurement setup for calibrating the RMS voltage of the PQ disturbance generator includes an NI USB-6218 DAQ device used to generate input voltage signals for the amplifier and a Fluke 8846A 6½-digit digital multimeter used to measure the amplifier's output RMS voltage values. The experimental system, which consists of the PQ disturbance generator, the NI USB-6218 DAQ device, and the Fluke 8846A reference multimeter, is depicted in Figure 4. The components of the measurement uncertainty budget for the RMS voltage of the generator are presented in Table 2. The PQ amplifier was calibrated using a FLUKE 5500A calibrator prior to the measurements, therefore its drift is not included in the uncertainty budget.

For calibration of the RMS voltage, six measurement points for the output of the PQ amplifier are taken: 230 V, 253 V, 207 V, 110 V, 121 V and 99 V. The warm-up time for the instruments is 1 h. The amplifier is set to the ±5 V input voltage range. Its amplification at this range is A = 79.554. The output of the DAQ device is set to a constant RMS value corresponding to the aforementioned measurement points (2.891 V, 3.18 V, 2.602 V, 1.383 V, 1.521 V and 1.244 V respectfully). The frequency of the generated voltage signal is 50 Hz and the signal is generated at a sampling rate of 25 kS/s. For each measurement point, $n = 10$ measurements are taken at five-minute time intervals between two successive measurements. The average measured voltage RMS values, as well as the calculated standard deviations for each measurement point are presented in Table 3.

Table 2. Measurement uncertainty components – RMS voltage.

Source	Type	Units	Notation	Sensitivity coefficients	Probability distribution	Divisor	Degrees of freedom
Standard deviation (repeatability)	A	V	$u_A(U)$	1	Normal	1	9
DMM accuracy	B	V	$u_{B1}(U)$	1	Uniform	$1/\sqrt{3}$	∞
DMM resolution	B	V	$u_{B2}(U)$	1	Uniform	$1/\sqrt{3}$	∞
DAQ accuracy	B	V	$u_{B3}(U)$	79.554	Uniform	$1/\sqrt{3}$	∞
DAQ resolution	B	V	$u_{B4}(U)$	79.554	Uniform	$1/\sqrt{3}$	∞

Table 3. Measurement results and calculated standard deviation (ST. DEV) – RMS voltage values.

	230 V U_{RMS} (V)	253 V U_{RMS} (V)	207 V U_{RMS} (V)	110 V U_{RMS} (V)	121 V U_{RMS} (V)	99 V U_{RMS} (V)
U_{avg} (n = 10)	229.4747	252.8879	207.4483	110.3206	121.4759	99.3593
ST. DEV	0.0698	0.0519	0.0417	0.0077	0.0437	0.0091
ST. DEV / $\sqrt{n}$	0.0221	0.0164	0.0132	0.0024	0.0138	0.0029

Table 4. Standard, combined and expanded measurement uncertainty values – RMS voltage.

Source	Standard uncertainty (V)					
	230 V	**253 V**	**207 V**	**110 V**	**121 V**	**99 V**
$u_A(U)$	$2.206 \cdot 10^{-2}$	$1.640 \cdot 10^{-2}$	$1.318 \cdot 10^{-2}$	$2.423 \cdot 10^{-3}$	$1.382 \cdot 10^{-2}$	$2.868 \cdot 10^{-3}$
$u_{B\text{-}DMM}(U)$	$2.527 \cdot 10^{-1}$	$2.608 \cdot 10^{-1}$	$2.451 \cdot 10^{-1}$	$2.114 \cdot 10^{-1}$	$2.153 \cdot 10^{-1}$	$2.076 \cdot 10^{-1}$
$u_{B\text{-}DAQ}(U)$	$9.134 \cdot 10^{-1}$	$9.210 \cdot 10^{-1}$	$9.064 \cdot 10^{-1}$	$8.845 \cdot 10^{-1}$	$8.863 \cdot 10^{-1}$	$8.828 \cdot 10^{-1}$
Combined uncertainty $u_C(U)$	$9.479 \cdot 10^{-1}$	$9.574 \cdot 10^{-1}$	$9.390 \cdot 10^{-1}$	$9.094 \cdot 10^{-1}$	$9.122 \cdot 10^{-1}$	$9.069 \cdot 10^{-1}$
Effective degrees of freedom $\nu_{eff}(U)$	$30.69 \cdot 10^{6}$	$104.43 \cdot 10^{6}$	$231.63 \cdot 10^{6}$	$17.86 \cdot 10^{10}$	$170.82 \cdot 10^{6}$	$9 \cdot 10^{10}$
Coverage factor k	1.96	1.96	1.96	1.96	1.96	1.96
Expanded uncertainty $u_{exp}(U)$	**1.858**	**1.876**	**1.840**	**1.782**	**1.788**	**1.777**

The calculation of the standard measurement uncertainty of the output RMS voltage of the PQ disturbance generator includes Type A uncertainty (standard deviation of the mean) and Type B uncertainty (DAQ device accuracy, DAQ device resolution, multimeter uncertainty and multimeter resolution). The standard deviation of the mean is calculated according to statistical methods applied on the measurement results, using the equation:

$$u_{\mathrm{A}}(U) = \sqrt{\frac{1}{n(n-1)}\sum_{i=1}^{n}\left(U_i - U_{\mathrm{avg}}\right)^2}. \tag{1}$$

Type B measurement uncertainties are calculated according to data and accuracies provided by the specifications of the applied instruments: digital multimeter Fluke 8846A [32] and DAQ device NI USB-6218 [33].

According to instrument specifications, the multimeter absolute uncertainty for the AC voltage range of 1000 V and frequency range from 10 Hz – 20 kHz is defined as $\Delta U_{\mathrm{DMM}} = \pm$ (0.06 % of measurement + 0.03 % of range). The multimeter resolution for the same range is $\Delta U_{\mathrm{DMM\text{-}res}} = 10$ mV, therefore the corresponding DMM Type B uncertainty $u_{B\text{-}DMM}(U)$ is calculated by:

$$u^2_{\mathrm{B-DMM}}(U) = u_{\mathrm{B1}}(U)^2 + u_{\mathrm{B2}}(U)^2 = \left(\frac{\Delta U_{\mathrm{DMM}}}{\sqrt{3}}\right)^2 + \left(\frac{1}{2}\frac{U_{\mathrm{DMM-res}}}{\sqrt{3}}\right)^2. \tag{2}$$

The output voltage signal of the PQ generator U_{out} is obtained by amplifying the voltage signal generated by the DAQ device U_{DAQ} and is calculated using equation (4). The amplifier's amplification A, for the ±5 V amplifier range is A = 79.554.

$$U_{\mathrm{out}} = A \cdot U_{\mathrm{DAQ}}. \tag{3}$$

The sensitivity coefficients for the Type B uncertainties of the DAQ device, c_3 and c_4, can be calculated using the following equation:

$$\frac{\partial U_{\mathrm{out}}}{\partial U_{\mathrm{DAQ}}} = A = c_3 = c_4. \tag{4}$$

Hence, the sensitivity coefficients c_3 and c_4 are equal to the amplifier's amplification. The nominal value of the PQ amplifier's amplification is $A = 80$, meaning that at the DAQ device's standardized output level of 5 V, the output RMS voltage from the amplifier would be equal to 400 V, which is necessary for PQ applications.

The absolute accuracy (which includes uncertainty due to drift) of the NI USB-6218 DAQ device U_{DAQ} is calculated using the method provided in the instrument specification, and the DAQ device resolution $U_{\mathrm{DAQ\text{-}res}}$ is calculated according to the DAC resolution of the device, $n_{\mathrm{DAC}} = 16$ bits and its output voltage range $U_r = \pm 10$ V = 20 V, as follows:

$$U_{\mathrm{DAQ-res}} = \frac{U_{\mathrm{r}}}{2^{n_{\mathrm{DAC}}} - 1}. \tag{5}$$

The corresponding DAQ device Type B uncertainty $u_{B\text{-}DAQ}(U)$ is calculated by using the following equation:

$$u^2_{\mathrm{B-DAQ}}(U) = c_3 u_3(U)^2 + c_4 u_4(U)^2 = A^2\left(\frac{\Delta U_{\mathrm{DAQ}}}{\sqrt{3}}\right)^2 + A^2\left(\frac{1}{2}\frac{U_{\mathrm{DAQ-res}}}{\sqrt{3}}\right)^2. \tag{6}$$

The combined voltage measurement uncertainty $u_C(U)$ is calculated using the previously calculated individual Type A and Type B uncertainties, as follows:

$$u_{\mathrm{c}}(U) = \sqrt{u_A(U)^2 + u_{\mathrm{B-DMM}}(U)^2 + u_{\mathrm{B-DAQ}}(U)^2}. \tag{7}$$

The number of overall effective degrees of freedom ν_{eff} for the combined uncertainty is calculated using the Welch-Satterthwaite equation:

$$\nu_{\mathrm{eff}} = \frac{u_{\mathrm{c}}(y)^4}{\sum_{i=1}^{N}\frac{c_i^4 u_i(x_i)^4}{\nu_i}}. \tag{8}$$

The number of effective degrees of freedom for the combined uncertainty of all six measurement points is a large number and can be considered as infinity ($\nu_{\mathrm{eff}} = \infty$).

The expanded measurement uncertainty of the PQ disturbance generator output RMS voltage $u_{\mathrm{exp}}(U)$ is calculated for a confidence interval of 95 %. The coverage factor that corresponds to this confidence interval and effective degrees of freedom $\nu_{\mathrm{eff}} = \infty$, adjusted according to the Student's t-distribution table is $k = 1.96$.

$$u_{\mathrm{exp}}(U) = k \cdot u_{\mathrm{c}}(U) = 1.96 \cdot u_{\mathrm{c}}(U). \tag{9}$$

The standard uncertainty for each of the uncertainty components, as well as the combined and expanded uncertainty for each of the measurement points are presented in Table 4. The expanded uncertainty is presented graphically in Figure 5.

The largest contributing component of the voltage RMS measurement uncertainty of the PQ disturbance generator is the Type B uncertainty of the DAQ device, $u_{B\text{-}DAQ}(U)$, due to the large sensitivity coefficient which is equal to the PQ signal amplifier's amplification. This component of the measurement uncertainty can be significantly reduced by using the PQ signal amplifier at its ±10 V range, thereby reducing its amplification as well as the Type B uncertainty of the DAQ device.

Table 5. Measurement uncertainty components – frequency.

Source	Type	Units	Notation	Sensitivity coefficients	Probability distribution	Divisor	Degrees of freedom
Standard deviation (repeatability)	A	Hz	$u_A(f)$	1	Normal	1	9
DMM accuracy	B	Hz	$u_{B1}(f)$	1	Uniform	$1/\sqrt{3}$	∞
DMM resolution	B	Hz	$u_{B2}(f)$	1	Uniform	$1/\sqrt{3}$	∞
DAQ accuracy	B	Hz	$u_{B3}(f)$	2500 at 50 Hz 3600 at 60 Hz	Uniform	$1/\sqrt{3}$	∞
DAQ resolution	B	Hz	$u_{B4}(f)$	2500 at 50 Hz 3600 at 60 Hz	Uniform	$1/\sqrt{3}$	∞

4.2. Frequency Uncertainty

The measurement setup for frequency calibration of the PQ disturbance generator is the same as the setup used for calibration of the voltage RMS and consists of the NI USB-6218 DAQ device used to generate the input voltage signals for the amplifier and a 6½-digit digital multimeter Fluke 8846A for measurement of the amplifier output frequency values. The components of the measurement uncertainty budget for the generator frequency are presented in Table 5.

For calibration of the frequency, two measurement points are taken: 50 Hz and 60 Hz. The amplifier is once again set to the ±5 V input voltage range. The output of the DAQ device is set to a constant RMS value: 2.891 V, corresponding to 230 V at the output of the amplifier. The signal is generated at a sampling rate of 25 kS/s. For each measurement point, 10 measurements are taken at five-minute time intervals between two successive measurements. The average measured frequency values and the calculated standard deviations for each measurement point are presented in Table 6.

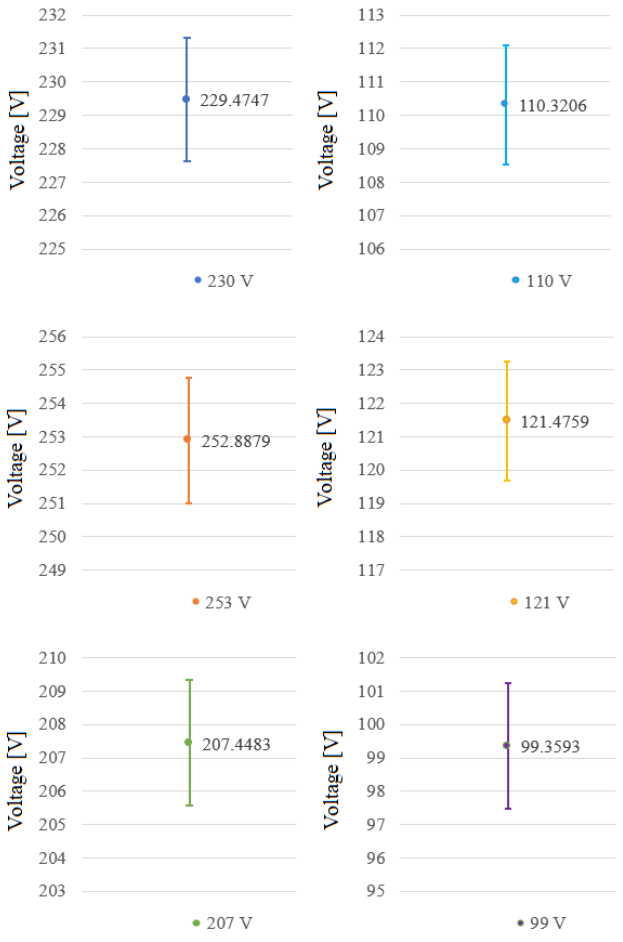

Figure 5. Graphical representation of the expanded uncertainty of the PQ generator – RMS voltage.

Similar to the measurement uncertainty of the output RMS voltage, the calculation of the standard measurement uncertainty of the frequency of the output voltage of the PQ disturbance generator includes Type A and Type B (DAQ device accuracy and resolution, multimeter uncertainty and resolution) uncertainty.

The standard deviation of the mean is calculated according to statistical methods applied on the measurement results, using the equation:

$$u_A(f) = \sqrt{\frac{1}{n(n-1)}\sum_{i=1}^{n}(f_i - f_{avg})^2}. \quad (10)$$

Type B measurement uncertainties are calculated according to data and accuracies provided by the specifications of the applied instruments. According to instrument specifications, the multimeter absolute uncertainty for the frequency range of 40 Hz – 300 kHz and RMS voltage range from 100 mV – 1000 V is defined as $\Delta f_{DMM} = \pm$ (0.01 % of measurement). The multimeter resolution for the same range is $f_{DMM\text{-}res} = 0.0001$ Hz, therefore the corresponding DMM Type B uncertainty $u_{B\text{-}DMM}(f)$ is calculated as:

$$u_{B-DMM}(f)^2 = u_{B1}(f)^2 + u_{B2}(f)^2 = \left(\frac{\Delta f_{DMM}}{\sqrt{3}}\right)^2 + \left(\frac{1}{2}\frac{f_{DMM-res}}{\sqrt{3}}\right)^2. \quad (11)$$

Type B measurement uncertainties of the DAQ device arise as a result of the timing accuracy and timing resolution of the device. According to the device specification, the timing accuracy is defined as ΔT_{DAQ} = (50 ppm of sample rate). The sampling rate $S_r = 25$ kS/s. The timing resolution of the DAQ device is $T_{DAQ\text{-}res} = 50$ ns. Because the timing accuracy and resolution are defined as units of time, the sensitivity coefficients for their respective uncertainties, c_3 and c_4 need to be determined. Equation (15) shows the dependence between the frequency of the generated signal f and its period T_{sig}:

$$f = \frac{1}{T_{sig}}. \quad (12)$$

Table 6. Measurement results and calculated standard deviations (ST. DEV) – PQ generator frequency values.

	50 Hz f (Hz)	60 Hz f (Hz)
f_{avg}	49.9992	59.9989
ST. DEV	$0.185 \cdot 10^{-3}$	$0.237 \cdot 10^{-3}$
ST. DEV / √n	$0.586 \cdot 10^{-4}$	$0.748 \cdot 10^{-4}$

Table 7. Standard, combined and expanded measurement uncertainty values – frequency.

Section	Standard Uncertainty (Hz)	
	50 Hz	60 Hz
$u_A(f)$	$5.859 \cdot 10^{-5}$	$7.483 \cdot 10^{-5}$
$u_{B\text{-}DMM}(f)$	$2.887 \cdot 10^{-3}$	$3.464 \cdot 10^{-3}$
$u_{B\text{-}DAQ}(f)$	$7.217 \cdot 10^{-2}$	$1.039 \cdot 10^{-1}$
Combined uncertainty $u_c(f)$	$7.223 \cdot 10^{-2}$	$1.040 \cdot 10^{-1}$
Effective degrees of freedom $\nu_{eff}(f)$	$2.08 \cdot 10^{13}$	$3.35 \cdot 10^{13}$
Coverage factor k	1.96	1.96
Expanded uncertainty $u_{exp}(f)$	$1.416 \cdot 10^{-1}$	$2.038 \cdot 10^{-1}$

The sensitivity coefficients for the Type B uncertainties of the DAQ device, c_3 and c_4, can be calculated using the following equation:

$$\frac{\partial f}{\partial T} = \frac{1}{T_{\text{sig}}^2} = f^2 = c_3 = c_4. \tag{13}$$

Hence, the sensitivity coefficients c_3 and c_4 are equal to the square of the generated signal's frequency.

The DAQ device Type B uncertainty $u_{B\text{-}DAQ}(f)$ is calculated as follows:

$$u_{\text{B-DAQ}}(f)^2 = c_3^2 u_{\text{B3}}(f)^2 + c_4^2 u_{\text{B4}}(f)^2 = +f^4 \left(\frac{T_{\text{DAQ}}}{\sqrt{3}}\right)^2 + f^4 \left(\frac{1}{2}\frac{T_{\text{DAQ-res}}}{\sqrt{3}}\right)^2. \tag{14}$$

The combined frequency measurement uncertainty $u_c(f)$ is calculated using the previously calculated individual Type A and Type B uncertainties, according to the following equation:

$$u_c(f) = \sqrt{u_A(f)^2 + u_{\text{B-DMM}}(f)^2 + u_{\text{B-DAQ}}(f)^2}. \tag{15}$$

The number of overall effective degrees of freedom ν_{eff} for the combined uncertainty is calculated using the Welch-Satterthwaite equation (8). The number of effective degrees of freedom for the combined uncertainty of both measurement points is a large number and can be considered as infinity ($\nu_{eff} = \infty$).

The expanded measurement uncertainty of the frequency of the PQ disturbance generator output voltage $u_{exp}(f)$ is calculated for a confidence interval of 95 %. The coverage factor that corresponds to this confidence interval and effective degrees of freedom $\nu_{eff} = \infty$, adjusted according to the Student's t-distribution table is $k = 1.96$.

$$u_{\text{exp}}(f) = k\, u_c(f) = 1.96 \cdot u_c(f). \tag{16}$$

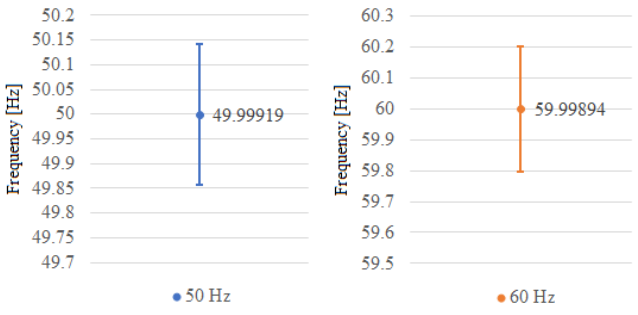

Figure 6. Graphical representation of the expanded uncertainty of the PQ generator – frequency.

The standard uncertainty for each of the uncertainty components, as well as the combined and expanded uncertainty for each of the measurement points are presented numerically in Table 7. The expanded uncertainty is presented graphically in Figure 6.

The relative measurement uncertainty of the frequency of the PQ disturbance generator for both measurement points is less than 0.5 %. The largest contributing component to the combined measurement uncertainty of the frequency is also the Type B uncertainty of the DAQ device $u_{B\text{-}DAQ}(f)$. This component can only be reduced by using a DAQ device with better timing accuracy and resolution.

When evaluating the frequency uncertainty of a PQ generator, higher order harmonics should be taken into account, however, within the scope of this paper, the authors limited the analysis only to the fundamental frequency.

Considering the metrological characteristics of the designed PQ generator obtained with its calibration, the system can be used as a PQ event simulator for research purposes and for testing and optimization of PQ event classifiers. However, in order to use this PQ generator as a reference instrument in testing PQ analyzers for example, its voltage and frequency measurement uncertainties need to be improved as per the recommendations stated in the preceding text.

5. CLASSIFICATION ACCURACY

For training purposes of the classifier, 21 classes of single and combined PQ disturbances are generated into a CSV file, 1000 signals per each class. The sampling frequency for all signals is 3.2 kHz and 10 cycles from every signal are included. The nominal frequency is 50 Hz.

Two types of pure signals are generated and reproduced for real-time classification. The first type consists of signals with same initial phases, which are commonly used in PQ classification research. However, the frequency in real power systems is almost never exactly equal to 50 Hz. This leads to each successive signal having a different initial phase. To address this, the second type of generated signals incorporate phase shift. To highlight the importance of the implemented zero-crossing detector, the classification is performed with and without zero-crossing detection. The obtained results are presented in Table 8.

The results show that when the generated voltage signals have the same initial phases, the classification accuracy is higher compared to cases with phase shift. This is due to the increased randomness introduced by the phase shift. When looking at the results for signals with phase shift, it becomes evident that the zero-crossing detector provides improved classification accuracy. The signals generated with phase shift using the proposed measurement setup are more representative of real measurements in the power grid compared to ideal voltage signals generated in MATLAB. For instance, the accuracy of the same classifier for pure signals generated in MATLAB using the signal generator presented in [34] is 96.48 % without phase shift and 94.72 % with phase shift and zero-crossing detection. However, it is worth noting that the accuracy of signals generated by the PQ generator is lower, as they are not ideal.

According to IEEE Std 1159-1995 [35], the measured signals contain noise with a typical voltage magnitude of 0-1 % of the nominal signal magnitude. To account for this, the experiment was repeated with noisy signals. The results, shown in Table 9, **reveal that the added noise increases the randomness of the** signals, leading to lower classification accuracy compared to the

results obtained with pure signals. The conclusion regarding phase shift remains unchanged, regardless of the presence of noise.

Results indicate that the PQ classifier has high classification accuracy, even when considering combinations of four different disturbances. This verifies the accuracy of the classifier and suggests that it is suitable for classifying real signals. The classification accuracy can be further improved by continually updating the training data with newly measured voltage signals. This will contribute to even more accurate classification of real voltage signals. Additionally, storing the raw measured signals will help to build a publicly accessible PQ database, which is currently scarce.

6. CONCLUSIONS

In this paper, two virtual instruments for power quality disturbance generation and real-time classification were presented. The proposed generator represents a virtual instrument for generating different PQ combinations according to the EN 50160 standard. The PQ classifier is trained to classify 21 classes of single and combined PQ disturbances. The main focus of the paper was to perform a metrological evaluation of the PQ generator and to verify the capability of the PQ classifier to classify disturbances in real-time.

For the metrological assessment of the realized PQ generator, a procedure for measurement uncertainty calculation was developed and presented. The results have shown that the relative measurement uncertainty of the PQ generator for all reference points is satisfactory. Thus, it can be used as a simulator of PQ signals for research purposes, for instance, for initial testing of PQ classifiers. However, the accuracy of the generator is not high enough to be used for testing of professional power monitoring equipment. The paper provides guidelines on how the measurement uncertainty can be improved.

Table 8. Classification accuracies obtained for pure signals.

PQ class	Without phase shift	With phase shift	
		Without zero-crossing	Without zero-crossing
D1	100.00%	100.00%	100.00%
D2	97.50%	91.40%	94.00%
D3	96.80%	93.10%	97.30%
D4	100.00%	97.50%	98.40%
D5	99.90%	98.30%	96.40%
D6	99.40%	97.50%	96.10%
D7	99.90%	97.20%	99.90%
D8	87.90%	78.70%	85.50%
D9	94.50%	91.00%	94.60%
D10	99.70%	99.70%	100.00%
D11	98.60%	97.80%	98.60%
D12	99.50%	99.20%	99.70%
D13	98.00%	86.70%	96.00%
D14	98.80%	87.40%	95.60%
D15	97.70%	94.80%	98.30%
D16	86.70%	80.50%	85.60%
D17	95.80%	91.80%	95.20%
D18	80.00%	64.90%	71.70%
D19	88.80%	81.70%	83.80%
D20	81.20%	70.90%	72.50%
D21	89.10%	81.10%	82.60%
Total	**94.75%**	**89.58%**	**92.47%**

Table 9. Classification accuracies obtained for signals accompanied by noise.

PQ class	Without phase shift	With phase shift	
		Without zero-crossing	Without zero-crossing
D1	99.60%	98.20%	98.90%
D2	88.50%	79.30%	85.60%
D3	95.60%	87.50%	95.30%
D4	97.90%	93.70%	95.40%
D5	97.80%	89.40%	90.50%
D6	98.80%	96.50%	95.60%
D7	99.80%	97.70%	99.70%
D8	81.80%	67.20%	78.60%
D9	93.80%	82.40%	92.10%
D10	99.90%	97.40%	98.00%
D11	88.30%	81.30%	84.60%
D12	96.20%	89.60%	95.70%
D13	95.20%	85.80%	90.30%
D14	99.00%	87.20%	94.60%
D15	97.80%	94.20%	97.20%
D16	74.80%	66.40%	71.30%
D17	92.00%	82.20%	91.60%
D18	73.90%	58.80%	66.60%
D19	87.10%	74.00%	81.60%
D20	72.90%	57.30%	61.30%
D21	86.30%	74.00%	79.60%
Total	**91.29%**	**82.86%**	**87.81%**

The accuracy of the classifier was verified by generating 21 classes of pure PQ disturbances and disturbances accompanied with noise. The results have confirmed that the implemented zero-crossing detector provides higher classification accuracy for signals with phase shift. Since the classifier works in real-time, the overall classification results have shown that it exhibits high classification accuracy even though in the classification process classes obtained as a combination of four disturbances are included. The proposed PQ signal generator and PQ classifier can be used for research purposes in the field of PQ analysis and for the development of decentralized real-time PQ monitoring systems.

REFERENCES

[1] Voltage characteristics of electricity supplied by public distribution systems, EN 50160:2010, European Committee for Electrotechnical Standardization (CENELEC), 2010.

[2] C. Tu, X. He, Z. Shuai, F. Jiang, Big data issues in smart grid – a review, Renewable & Sustainable Energy Reviews 79 (2017), pp. 1099-1107. DOI: 10.1016/j.rser.2017.05.134

[3] W. E. Brumsickle, D. M. Divan, G. A. Luckjiff, J. W. Freeborg, R. L. Hayes, Operational experience with a nationwide power quality and reliability monitoring system, 38th IAS Annual Meeting on Conference Record of the Industry Applications Conference, 2003., Salt Lake City, UT, USA, 2003, pp. 1063-1067. DOI: 10.1109/IAS.2003.1257679

[4] P. Daponte, M. Di Penta, G. Mercurio, TransientMeter: a distributed measurement system for power quality monitoring, IEEE Trans. Power Deliv. 19(2) (2004), pp. 456-463. DOI: 10.1109/TPWRD.2004.825200

[5] D. Divan, G.A. Luckjiff, W.E. Brumsickle, J. Freeborg, A. Bhadkamkar, A grid information resource for nationwide real-time power monitoring, IEEE Trans. Ind. Appl. 40(2) (2004), pp. 699-705. DOI: 10.1109/TIA.2004.824503

[6] P. K. Lee, L. L. Lai, A practical approach to wireless GPRS on-line power quality monitoring system, 2007 IEEE PES General Meeting, Tampa, FL, USA, 2007, pp. 1-7. DOI: 10.1109/PES.2007.385937
[7] P. K. Lee, L. L. Lai, A practical approach to wireless Power Quality, Energy and Facilities Monitoring System, 2008 IEEE PES General Meeting - Conversion and Delivery of Electrical Energy in the 21st Century, Pittsburgh, PA, USA, 2008, pp. 1-3. DOI: 10.1109/PES.2008.4596413
[8] C. Kocatepe, B. Kekezoğlu, A. Bozkurt, R. Yumurtaci, A. İnan, O. Arikan, M. Baysal, Y. Akkaya, Survey of power quality in Turkish national transmission network, Turkish Journal of Electrical Engineering & Computer Sciences 21 (2013), pp. 1880-1892. DOI: 10.3906/elk-1201-21
[9] S. Di Pasquale, S. Giarnetti, F. Leccese, D. Trinca, M. Cagnetti, M. Caciotta, A distributed web-based system for temporal and spatial power quality analysis, in: Power Quality Issues in Distributed Generation. J. Luszcs (editor), IntechOpen, London, 2015, ISBN 978-953-51-6392-3, pp. 127-145.
[10] L. Cristaldi, A. Ferrero, S. Salicone, A distributed system for electric power quality measurement, IEEE Trans. Instrum. Meas. 51(4) (2002), pp. 776-781. DOI: 10.1109/TIM.2002.803300
[11] S.-J. S. Tsai, C. C. Luo, Synchronized power-quality measurement network with LAMP, IEEE Trans. Power Deliv. 24(1) (2009), pp. 484-485. DOI: 10.1109/TPWRD.2008.2005361
[12] A. Carta, N. Locci, C. Muscas, GPS-based system for the measurement of synchronized harmonic phasors, IEEE Trans. Instrum. Meas. 58(3) (2009), pp. 586-593. DOI: 10.1109/TIM.2008.2005075
[13] M. R. Sindhu, G. N. Manjula, T. N. P. Nambiar, Development of LabVIEW based harmonic analysis and mitigation scheme with shunt active filter for power quality enhancement, Int. J. Recent Technology and Engineering 2(5) (2013), pp. 71-78.
[14] T. Demirci. A. Kalaycioglu, D. Küçük (+ another 9 authors), Nationwide real-time monitoring system for electrical quantities and power quality of the electricity transmission system, IET Generation, Transmission & Distribution 5(5) (2011), pp. 540-550. DOI: 10.1049/iet-gtd.2010.0483
[15] J. J. G. de la Rosa, A. Agüera-Pérez, J. C. Palomares-Salas, J. M. Sierra-Fernández, A. Moreno-Muñoz, A novel virtual instrument for power quality surveillance based in higher-order statistics and case-based reasoning, Measurement 45(7) (2012), pp. 1824–1835. DOI: 10.1016/j.measurement.2012.03.036
[16] R. Saxena, A. K. Swami, S. Mathur, A power quality signal generator in LabVIEW environment, Int. Conf. Advances in Electronics, Electrical and Computer Science Engineering – EEC 2012, Dehradun, Uttarakhand, India, 2012, pp. 36–39.
[17] W. Zhu, W. Y. Ma, Y. Gui, H. F. Zhang, Modelling and simulation of PQ disturbance based on Matlab, International Journal of Smart Grid and Clean Energy 2 (2013) 1, pp. 18–24. DOI: 10.12720/sgce.2.1.18-24
[18] S. Caldara, S. Nuccio, C. Spataro, IEEE Trans. Instrum. Meas. 47(5) (1998), pp. 1155-1158. DOI: 10.1109/19.746574
[19] Y. Huping, B. Zhipeng, The power quality monitoring system based on virtual instrument, 2009 WRI World Congress on Software Engineering, Xiamen, China, 2009, pp. 243–245. DOI: 10.1109/WCSE.2009.47
[20] M. Markovska, D. Taskovski, Z. Kokolanski, V. Dimchev, B. Velkovski, Real-time implementation of optimized power quality events classifier, IEEE Trans. Ind. Appl. 56(4) (2020), pp. 3431–3442. DOI: 10.1109/TIA.2020.2991950
[21] E. G. Ribeiro, T. M. Mendes, G. L. Dias, E. R. S. Faria, F. M. Viana, B. H. G. Barbosa, D. D. Ferreira, Real-time system for automatic detection and classification of single and multiple power quality disturbances, Measurement 128 (2018), pp. 276-283. DOI: 10.1016/j.measurement.2018.06.059
[22] M. H. Bollen, K. Stockman, R. Neumann, G. Ethier, J. Romero Gordon, K. van Reussel, S. Z. Djokic, S. Cundeva, Voltage dip immunity of equipment and installations – messages to stakeholders, 2012 IEEE 15th Int. Conf. Harmonics and Quality of Power, Hong Kong, China, 2012, pp. 915-919. DOI: 10.1109/ICHQP.2012.6381173
[23] M. Simić, Z. Kokolanski, D. Denić, V. Dimcev, D. Živanović, D. Taskovski, Design and evaluation of computer-based electrical power quality signal generator, Measurement 107 (2017), pp. 77-88. DOI: 10.1016/j.measurement.2017.05.010
[24] B. Velkovski, Z. Kokolanski, A virtual signal generator for real-time generation of power quality disturbances, 2020 XXIX Int. Sci. Conf. Electronics (ET), Sozopol, Bulgaria, 2020, pp. 1-4. DOI: 10.1109/ET50336.2020.9238243
[25] Z. Kokolanski, C. Gavrovski, I. Mircevska, V. Dimcev, M. Simic, On the design of power quality signal amplifier, 2016 XXV Int. Sci. Conf. Electronics (ET), Sozopol, Bulgaria, 2016, pp. 1-4. DOI: 10.1109/ET.2016.7753491
[26] V. Dimcev, D. Taskovski, Z. Kokolanski, D. Denic, D. Zivanovic, M. Simic, Signal conditioning for power quality, 11th Int. Conf. Electrical Power Quality and Utilisation, Lisbon, Portugal, 2011, pp. 1-5. DOI: 10.1109/EPQU.2011.6128809
[27] Electromagnetic compatibility (EMC), Part 4-30: Testing and measurement techniques - Power quality measurement methods, IEC 61000-4-30:2015+AMD1:2021, IEC, 2021.
[28] M. Markovska. D. Taskovski, The effectiveness of wavelet-based features on power quality disturbances classification in noisy environment, 2018 18th Int. Conf. Harmonics and Quality of Power (ICHQP), Ljubljana, Slovenia, 2018, pp. 1-6. DOI: 10.1109/ICHQP.2018.8378873
[29] M. Markovska, D. Taskovski, On the choice of optimal method for feature extraction and classification of voltage disturbances, J. Electr. Eng. and Inf. Technol. 4(2) (2019), pp. 15-27. DOI: 10.51466/JEEIT1941-2015m
[30] Uncertainty of measurement – Part 3: Guide to the expression of uncertainty in measurement (GUM:1995), ISO/IEC Guide 98-3:2008, 2008.
[31] C. Papadopoulos, H. Yeung, Uncertainty estimation and Monte Carlo simulation method, Flow Measurement and Instrumentation 12(4) (2001), pp. 291-298. DOI: 10.1016/S0955-5986(01)00015-2
[32] Fluke 8845A/8846A DMM user's manual, Fluke Corp., 2006. Online [Accessed 24 June 2023] https://assets.fluke.com/manuals/884xa___umeng0200.pdf
[33] NI USB-6218 Specifications, NI Corp., 2017. Online [Accessed 15 June 2023] https://www.ni.com/docs/en-US/bundle/usb-6218-specs/page/specs.html
[34] R. Igual, C. Medrano, F. J. Arcega, G. Mantescu, Integral mathematical model of power quality disturbances, 2018 18th Int. Conf. Harmonics and Quality of Power (ICHQP), Ljubljana, Slovenia, 2018, pp. 1-6, DOI: 10.1109/ICHQP.2018.8378902
[35] IEEE recommended practice for monitoring electric power quality, IEEE Std. 1159-1995, 1995. DOI: 10.1109/IEEESTD.1995.79050